



Research paper

NRAMP1 promotes iron uptake at the late stage of iron deficiency in poplars

Hui-Min Chen^{1,2,4}, Yi-Ming Wang³, Hai-Ling Yang³, Qing-Yin Zeng^{1,2,4}, Yan-Jing Liu^{1,2,5}

¹State Key Laboratory of Tree Genetics and Breeding, Chinese Academy of Forestry, Beijing 100091, China; ²State Key Laboratory of Systematic and Evolutionary Botany, Institute of Botany, Chinese Academy of Sciences, Beijing 100093, China; ³College of Biological Sciences and Biotechnology, Beijing Forestry University, Beijing 100083, China; ⁴University of Chinese Academy of Sciences, Beijing 100049, China; ⁵Corresponding author (yan.jing.liu@163.com) orcid.org/0000-0002-1986-543X

Received December 6, 2018; accepted May 10, 2019; handling Editor Torgny Näsholm

Iron (Fe) is an essential micronutrient for plant survival and proliferation. Plants have evolved complex mechanisms to maintain Fe homeostasis in response to Fe deficiency. In this study, we evaluated the physiological, biochemical and transcriptomic differences between poplars grown under Fe-sufficient and Fe-deficient conditions to elucidate the mechanistic responses of poplars to Fe deficiency. Our results revealed that chlorophyll synthesis and photosynthesis were inhibited under Fe-deficient conditions. The inhibition of these pathways caused chlorosis and reduced shoot growth. Although both photosynthetic systems (PSI and PSII) were inhibited under Fe limitation, PSI was affected more severely and earlier than PSII. Fe deficiency also promoted root growth and increased the accumulation of divalent metal ions in roots. IRT1 and NRAMP1 are both Fe²⁺ transporters for iron uptake in *Arabidopsis*. In this study, however, only NRAMP1 was induced to promote Fe²⁺ uptake in roots at the late stage of Fe deficiency response. It indicated that NRAMP1, rather than the more well-known IRT1, might be a major Fe²⁺ transporter at the late stage of Fe-deficiency in poplars.

Keywords: Fe²⁺ transporter, iron deficiency, NRAMP1, poplars.

Introduction

Iron (Fe) is an essential element for plant growth and development (Kobayashi and Nishizawa 2012, Briat et al. 2015). As a cofactor of numerous redox proteins, Fe participates in many crucial metabolic pathways in plants, such as chlorophyll synthesis, photosynthesis, respiration and peroxidase system (Colangelo Aksoy et al. 2013). However, plants often face significant challenges in maintaining Fe homeostasis due to the low level of soluble Fe in calcareous soil. Fe deficiency causes chlorosis and retards growth in plants (Toselli et al. 2000). To adapt to Fe-limited environment, nongraminaceous plants such as *Arabidopsis* have evolved an effective reduction strategy for Fe acquisition through three stages (Marschner et al. 1986). First, protons (H⁺) are extruded to acidify the rhizosphere and release soluble Fe³⁺ from insoluble hydroxide complexes. In *Arabidopsis*, two H⁺-ATPases, AtAHA2 and AtAHA7, are

involved in proton secretion (Gao and Chao 2016). Next, Fe³⁺ is reduced to Fe²⁺ by ferric chelate reductase (FCR). Ferric reduction oxidase 2 (FRO2) is a protein located on the membranes of root epidermal cells (Einset et al. 2008). Under Fe shortage, FRO2 is induced to reduce Fe³⁺ to Fe²⁺. The overexpression of *AtFRO2* can increase the tolerance to Fe deficiency in transgenic *Arabidopsis* plants (Robinson et al. 1999, Curie and Briat 2003). Finally, the reduced Fe²⁺ is transported into root cells by Fe²⁺ transporters. Iron-regulated transporter 1 (AtIRT1) is a major Fe²⁺ transporter with a strong affinity for Fe²⁺ (Varotto et al. 2002). AtIRT1 has been shown to be strongly induced within 3 days of Fe deficiency (Yang et al. 2010, Colangelo Aksoy et al. 2013, Hindt et al. 2017, Hirayama et al. 2018). Natural resistance-associated macrophage 1 (NRAMP1) is another Fe²⁺ transporter located on the plasma membrane. AtNRAMP1 cooperates with AtIRT1

to take up Fe²⁺ in *Arabidopsis* roots (Curie et al. 2000, Castaings et al. 2016).

The redistribution of Fe in plants is another way to regulate Fe homeostasis. Because vacuole is a major Fe repository, plants can use the Fe in vacuoles to sustain cytoplasmic metabolism when Fe is limited. Under Fe-limited conditions, the expression of *AtNRAMP3* and *AtNRAMP4*, which code for proteins that transport Fe from the vacuole to the cytosol, is upregulated (Thomine et al. 2003, Lanquar et al. 2005). Meanwhile, the expression of vacuolar iron transporter 1 (*AtVIT1*) and cation-chloride co-transporter 1 like (*CCC1-like*), which code for proteins that transport Fe from cytosol to vacuole is downregulated (Gollhofer et al. 2011, Gollhofer et al. 2014). The long-distance Fe transporter genes, such as yellow stripe-like (*YSLs*) and oligopeptide transporter gene 3 (*OPT3*), are also involved in Fe redistribution. In *Arabidopsis*, *AtYSL1* and *AtYSL3* accumulate Fe into sink tissues and are downregulated during low-Fe conditions (Waters et al. 2006). *AtOPT3* transports Fe to developing tissues. The gene encodes *AtOPT3* is upregulated during Fe deficiency (Zhai et al. 2014).

Several regulators that participate in the response to Fe deficiency have been identified. The FER-like iron deficiency-induced transcription factor (FIT) are major positive regulators of Fe homeostasis (Ivanov et al. 2012). Tomato *LeFER1* positively regulates Fe starvation by inducing the expression of *LeIRT1* and *LeNRAMP1* (Ling et al. 2002). In *Arabidopsis*, *AtFIT1* (*AtbHLH29*) interacts with the Ib subgroup protein of the bHLH superfamily (*AtbHLH38/39/100/101*) to form a heterodimer (Yuan et al. 2008, Wang et al. 2013). Under low-Fe conditions, the expression of *AtbHLH38/39/100/101* and *AtFIT1* are all upregulated. The heterodimers of their encoding proteins induced the expression of *AtFRO2* and *AtIRT1* (Colangelo and Guerinot 2004, Yuan et al. 2008, Wang et al. 2013). Furthermore, ethylene is a signal molecule that positively regulates responses to Fe deficiency (Garcia et al. 2010). Ethylene insensitive 3 (EIN3) and ethylene insensitive 3-like 1 (EIL1) are transcription factors involved in the ethylene signaling pathway. EIN3 and EIL1 interact with FIT to maintain FIT accumulation (Lingam et al. 2011). POPEYE (PYE) is another transcription factor involved in the response to Fe deficiency (Ivanov et al. 2012). Four PYE-like proteins, bHLH34, bHLH104, bHLH105 (IAA-LEUCINE RESISTANT3, ILR3) and bHLH115, regulate Fe homeostasis by forming homo- or heterodimers (Long et al. 2010, Li et al. 2016). Under Fe-deficient conditions, upregulation of the *AtPYE* promotes root growth and inhibits the expression of several metal homeostasis genes, including *AtFRO3*, *AtNAS4* and *AtZIP1* (Long et al. 2010). *AtPYE* and *AtbHLH38/39/100/101* are activated by *AtbHLH34*, *AtbHLH104* and *AtbHLH105* (Li et al. 2016). *AtbHLH104* and *AtbHLH105* are negatively regulated by *AtBTS* (*BRUTUS*), which is co-expressed with *PYE* in response to Fe deficiency (Ivanov et al. 2012, Zhang et al. 2015). *AtBTS* interact with *AtbHLH104* and *AtbHLH105* to

promote their degradation via a 26S proteasome pathway (Long et al. 2010, Selote et al. 2015).

In poplars, the genes involved in Fe uptake and Fe homeostasis have been reported (Huang and Dai 2015a, 2015b). However, little is known about the regulatory mechanism in response of Fe deficiency in poplars. In this study, we investigated the physiological, biochemical and transcriptomic changes that occur during Fe deficiency in poplars and elucidated the mechanism of the late-stage response to Fe deficiency.

Materials and methods

Plant culture, Fe treatment and RNA-seq

Individuals of hybrid poplar clone 741 (*Populus alba* × (*Populus davidiana* + *Populus simonii*) × *Populus tomentosa*) were micropropagated on 5% agar-solidified Lloyd & McCown woody plant basal medium (WPM) with 1.5% sucrose and 1 mg/L naphthaleneacetic acid. The growth chamber conditions were set as follows: 24°C, 16 h of light per day and photon flux density of ~50 μmol m⁻² s⁻¹. After 4 weeks of micropropagation, the plants at the same developmental stage (~10 cm shoot length) were selected and transferred into WPM solution. After another 3 days in the hydroponic solution, the plants were divided into two groups. The control group was transferred to new WPM solution containing 100 μM Fe (Fe sufficient), and the treatment group was transferred to new WPM solution containing 0 μM Fe (Fe deficient). The Fe-deficient plants grew normally initially. We considered this to be the early stage of Fe deficiency. After 15 days, the young leaves of Fe-deficient plants were visibly chlorotic, indicating that the plants had entered the late stage of Fe deficiency. Control and treatment plants were then harvested for morphological, physiological and biochemical analyses, and their roots were collected for RNA-seq. The shoots from both groups were also sampled and isolated from cultured plants after 15 days' treatment. RNA isolation, library construction and sequencing were carried out at Biomarker Technologies (Beijing, China) using three biological replicates.

Measurement of morphological parameters and FCR activity

Seven replicates from each group were used to measure morphological parameters. The roots of each sample were placed in a dish containing water so that the roots were well dispersed and easy to measure. Six replicates from each group were used to quantify FCR activity, following the protocol from Jin et al. (2007).

Quantification of sample elemental content

The roots, stems and leaves of each sample were dried in an oven at 80°C until a constant weight was reached. The dried samples were then ground to powder. Subsequently, 0.1–0.2 g of each powdered sample was placed in a digestion tube with 6 ml nitric acid and digested using a microwave system. The digested samples were diluted to 50 ml with distilled water, and Fe, manganese (Mn), copper (Cu) and zinc (Zn) contents

were determined by inductively coupled plasma optical emission spectrometer (ICP-AES, iCAP6300, Thermo, USA). Four replicates were analyzed per group.

Quantification of photosynthetic pigment levels

The third leaf of each plant was cut up and soaked in 80% acetone to extract photosynthetic pigments, and the extract was centrifuged at $5300 \times g$ for 10 min. The absorbance of the supernatant was then read at 647, 645 and 663 nm using the Evolution™ 300 UV-Vis Spectrophotometer (Thermo). Total chlorophyll, chlorophyll *a*, chlorophyll *b* and carotenoid concentrations were calculated using methods described by Bruinsma (1963). Six replicates were analyzed per group.

Measurement of photosynthetic parameters

The P700 absorbance (representing photosystem I [PSI]) and chlorophyll fluorescence (representing photosystem II [PSII]) of the third leaf of each plant were measured according to the manufacturer's instructions using the Dual-PAM-100 system (Walz, Germany). Four replicates were measured per group. The GFS-3000 portable photosynthesis system (Walz, Germany) was used to measure the gas exchange parameters, such as the net photosynthetic rate (*A*), stomatal conductance (g_{H_2O}), transpiration rate (*E*) and intercellular carbon dioxide concentration (*C_i*), of the third leaves. Measurements were conducted according to the manufacturer's instructions. Four replicates were measured per group.

Statistical analysis

Independent *t*-test were used to compare the morphological parameters, FCR activity, elemental content, levels of photosynthetic pigments and photosynthetic parameters between control and Fe-deficient groups. The *P*-values for all parameters were pooled together and controlled for the false discovery rates (FDR) using the qvalue (Storey et al. 2015) R package. Significant differences at *P* < 0.05 and *P* < 0.01 (FDR ≤ 0.05) were indicated using * and **, respectively.

RNA-seq analysis

Raw reads were filtered to obtain clean reads using NGSToolkit (V2.3.3) and Trimmomatic (V0.36) software. The filtering criteria are as follows: (i) reads containing adapters, (ii) reads with more than 10% unknown bases or (iii) reads with more than 50% of total bases with quality values ≤ 20 were removed. The clean reads were aligned with the *Populus trichocarpa* genome obtained from Phytozome V12.1 (<https://phytozome.jgi.doe.gov>) using the HISAT (V2.0.5) software with default parameters. The reads that mapped to transcripts were quantified using HTSeq (V2.2.1). The differentially expressed genes (DEGs) were identified using the edgeR package (V3.16.5). Genes with an absolute fold change (FC) ≥ 2 ($|\log_2$ fold change (FC)| ≥ 1) and an FDR < 0.05 were considered differentially expressed. Gene ontology (GO) annotation was performed using Blast2GO

(V4.0). GO enrichment analysis of the DEGs was conducted using the topGO (V2.30.0). The Kyoto Encyclopedia of Genes and Genomes (KEGG) enrichment analysis of the DEGs was conducted using KOBAS (V2.0). KEGG pathway mapping of the DEGs was carried out using the online KEGG Automatic Annotation Server (KAAS; <http://www.genome.jp/kegg/kaas>). The differentially expressed transcription factors (DETFs) were predicted using the PlantTFdb online tool (<http://planttfdb.cbi.pku.edu.cn/>). The protein interaction network was elucidated using the online STRING tool (<http://string-db.org/>). High-throughput sequence data generated from this study have been deposited in the Gene Expression Omnibus (GEO) database under accession number GSE116838.

Validation using quantitative real-time polymerase chain reaction

Total RNA was extracted from each sample using the TIANGEN Polysaccharides & Polyphenolics-rich Total RNA extraction kit (TIANGEN BIOTECH, Beijing, China). We checked the concentration and quality of the extracted RNA using the Nanodrop 2000 spectrophotometer (Thermo) and agarose gel electrophoresis. The extracted RNA was reverse transcribed to cDNA using the Takara RNA PCR kit (AMV; Takara Bio Inc., Mountain View, CA, USA). Six DEGs common to the roots and shoots were selected for validation with quantitative real-time polymerase chain reaction (qRT-PCR), using the conserved *ACTIN* as a reference gene. Primer Express (V5.0) was used to design the primers for these DEGs (see Table S1 available as Supplementary Data at *Tree Physiology Online*). Using the cDNA strand of each sample as a template, PCR amplification was carried out in the StepOnePlus™ Real-Time PCR System (Applied Biosystems, Foster City, CA, USA) with the designed primers and SYBR® Premix Ex Taq™ II (Takara Bio Inc.). Relative expression levels were calculated using the $2^{-\Delta\Delta CT}$ method (Livak and Schmittgen 2001). Three independent biological replicates and three technical replicates were analyzed in this experiment.

Results

Fe deficiency induced leaf chlorosis and the accumulation of non-Fe divalent metal ions in poplar roots

Under Fe deficiency, the top leaves of each plant exhibited visible intercostal chlorosis (Figure 1A). The mean shoot height of the Fe-deficient plants was 11.54% lesser than that of control plants, whereas the mean root length and root number of Fe-deficient plants were 40.00% and 112.24% greater, respectively, than those of control plants (Figure 1B). Divalent Fe, Mn, Cu and Zn contents in the leaves, stems and roots were investigated (Figure 2). Fe content in the roots, stems and leaves of Fe-deficient plants was significantly lower than that in control plants, with decreases of 78.53%, 23.28% and 48.08%, respectively. Conversely, Mn, Cu and Zn content

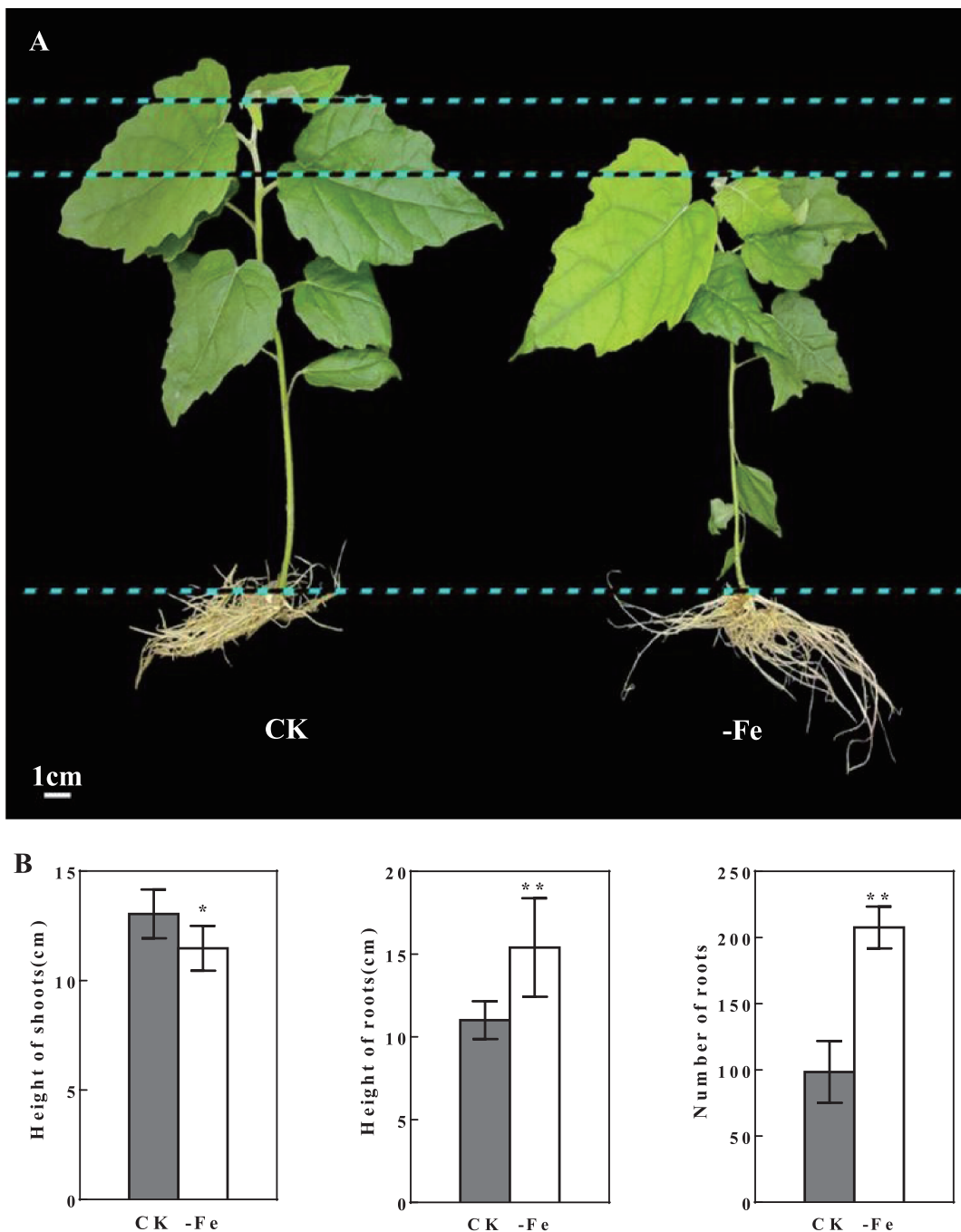


Figure 1. Effects of iron deficiency on poplar morphology. (A) Morphological and (B) growth parameters in control (CK) and iron-deficient ($-Fe$) plants; $n = 7$. Data were collected on day 15 of treatment. ** $P < 0.01$ and * $P < 0.05$, treatment vs. control (t -test, FDR < 0.05).

in the roots of Fe-deficient plants was significantly higher by 373.03%, 52.03% and 100.89%, respectively. No significant difference in Mn, Cu or Zn content was found between control and treatment leaves and stems.

Photosynthetic pigment contents and photosystem were influenced by Fe deficiency

Chlorophyll and carotenoid concentrations in the leaves were investigated (Figure 3A). Chlorophyll *a*, chlorophyll *b* and

carotenoid concentrations were 48.67%, 48.03% and 37.10% lower, respectively, in Fe-deficient leaves. However, the ratio of chlorophyll *a* to *b* did not differ significantly between control and treatment leaves. P700 absorbance (PSI) and chlorophyll fluorescence (PSII) were measured on days 15 and 30 of treatment (Figure 3B and C). On day 15, the PSI photochemical quantum yield ($Y_{[I]}$) and relative electron transfer efficiency (ETR $[I]$) of Fe-deficient leaves were 38.50% and 35.70% lower, respectively, than those of control leaves. The receptor-side

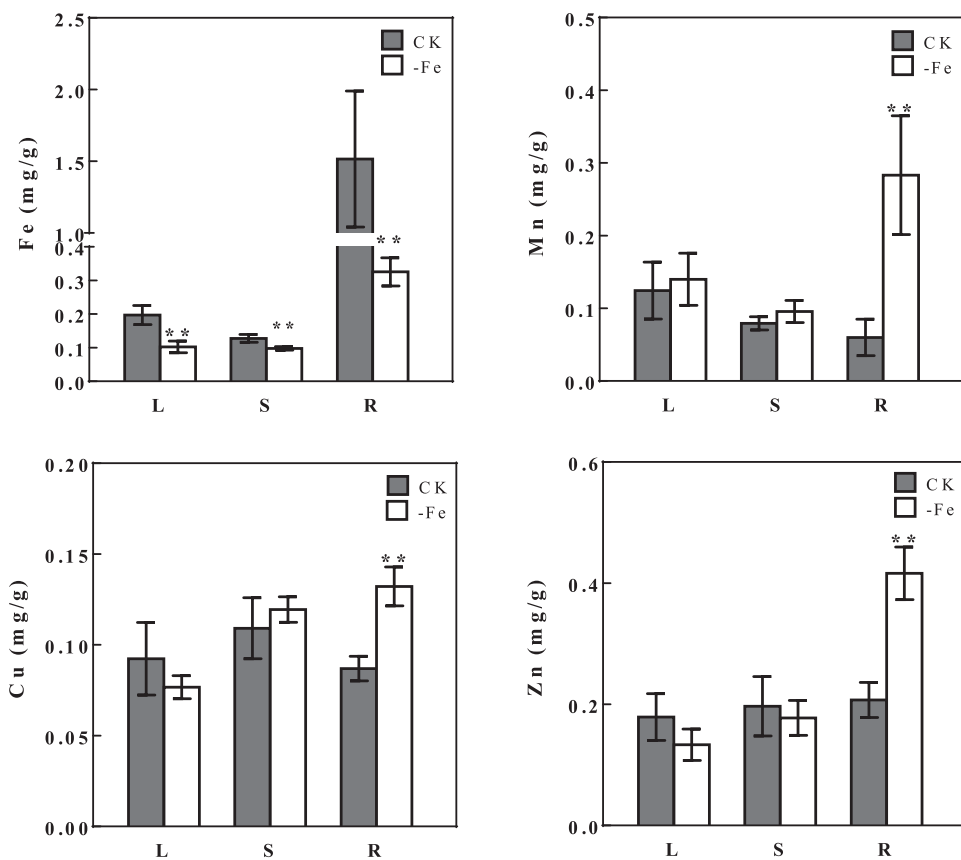


Figure 2. Effects of iron deficiency on elemental content in poplars. CK, control; -Fe, Fe-deficient; L, leaf; S, stem; R, root; $n = 4$. Data were collected on day 15 of treatment. ** $P < 0.01$, treatment vs. control (t -test, FDR < 0.05).

non-photochemical quantum yield (Y [NA]) of Fe-deficient leaves was significantly higher (by 176%) than that of control leaves. In contrast, the donor-side non-photochemical quantum yield (Y [ND]), which is regulated by PSII activity levels, of Fe-deficient leaves decreased by 87.75%, but this difference was not significant due to the large variance in control measurements ($P = 0.19$, t -test, FDR = 0.30). On day 30, Y (I), ETR (I), Y (NA) and Y (ND) differed significantly between the control and treatment groups. The Y (I) and ETR (I) of Fe-deficient leaves were 45.53% and 41.77% lower, respectively, whereas the Y (NA) and Y (ND) of Fe-deficient leaves were 7.24-fold and 381.67-fold higher, respectively. In terms of PSII activity, only Fv/Fm (maximum potential light energy conversion efficiency of PSII) in Fe-deficient leaves was significantly lower, by 5.83%, on day 15 compared with control leaves. The Y (II), ETR (II) and quantum yield of non-regulated energy dissipation (Y [NO]) and quantum yield of regulated non-photochemical energy loss (Y [NPQ]) in PSII all had no significant difference between the treatment and control. On day 30, the Fv/Fm , Y (II) and ETR (II) of Fe-deficient leaves were significantly lower than control measurements, by 28.08%, 40.91% and 40.82%, respectively. In contrast, the Y (NO) and Y (NPQ) of Fe-deficient leaves were significantly

higher than control measurements, by 72.78% and 141.33%, respectively.

On day 15, Y (I), ETR (I) and Y (NA) values differed significantly between the treatment and control, indicating that PSI activity had been inhibited. For PSII, only Fv/Fm was significantly lower in treatment leaves, indicating that PSII activity was depressed, but not as severely as in PSI. Therefore, Fe deficiency affected PSI earlier than PSII. The PSI and PSII activities were significantly inhibited with the onset of severe chlorosis.

Gas exchange parameters were also measured (Figure 3D). The net photosynthetic rate (A), transpiration rate (E) and stomatal conductance (g_{H2O}) were significantly lower in Fe-deficient leaves than in control leaves, by 69.36%, 47.82% and 50.57%, respectively. However, the intercellular carbon dioxide concentration (C_i) was 9.41% higher in Fe-deficient leaves than in control leaves. Our results confirm that Fe deficiency greatly influences photosynthesis in poplars.

Analysis of DEGs in shoots and roots

Based on our screening criteria, 361 and 641 DEGs were identified in the shoots and roots, respectively (Figure 4A). Of the 361 shoot DEGs, 232 genes were upregulated and 129 genes were downregulated. Of the 641 root DEGs, 266 genes were

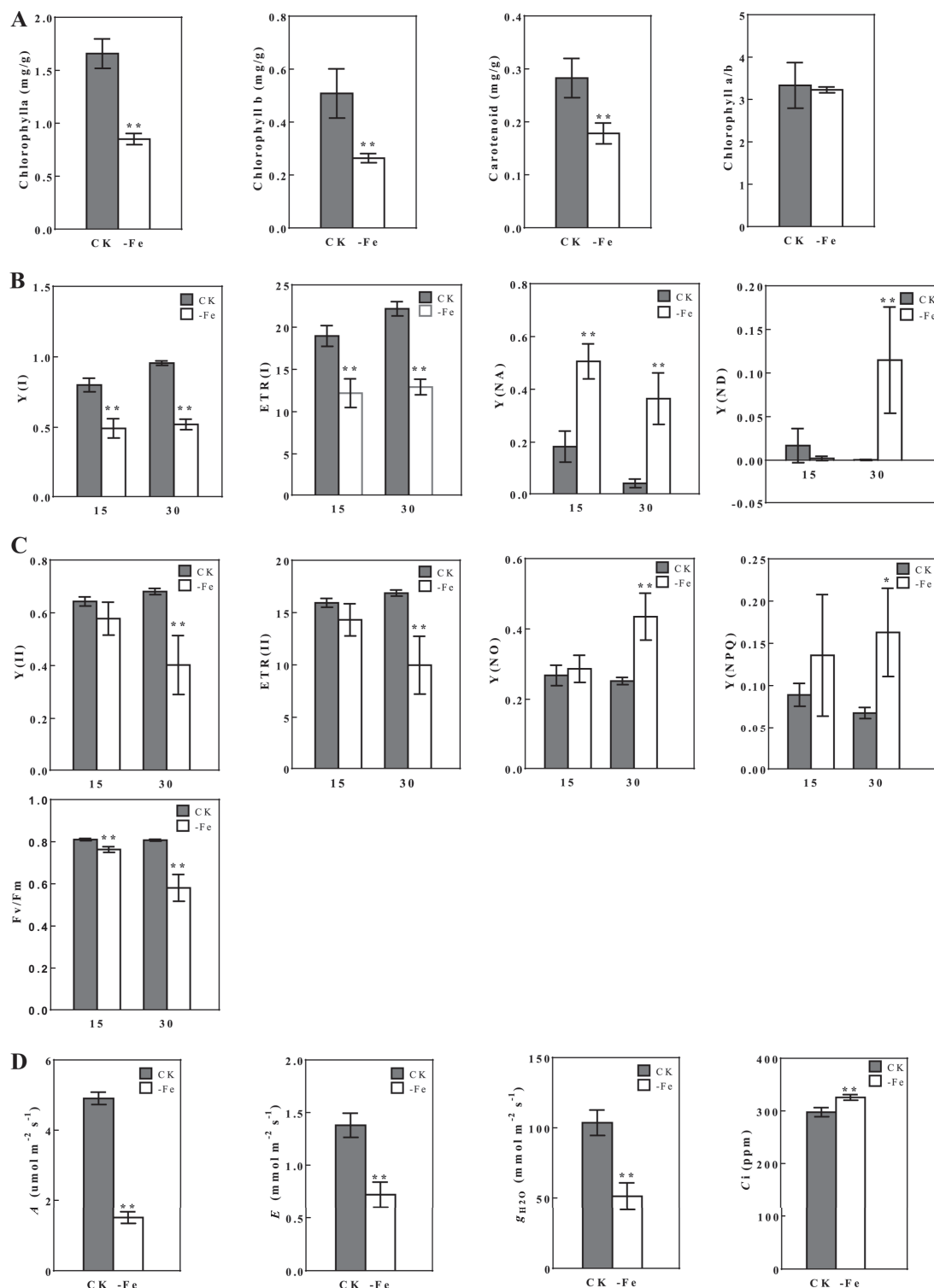


Figure 3. Effects of iron deficiency on levels of photosynthetic pigments and photosynthetic parameters in poplars. (A) Effects on levels of photosynthetic pigments; $n = 6$. Data were collected on day 15 of treatment. (B) Effects on PSI. $Y(I)$, PSI photochemical quantum yield; $ETR(I)$, PSI relative electron transfer efficiency; $Y(NA)$, receptor-side non-photochemical quantum yield; $Y(ND)$, donor-side non-photochemical quantum yield, regulated by PSII activity; $n = 4$. Data were collected on days 15 and 30 of treatment. (C) Effects on PSII. $Y(II)$, PSII photochemical quantum yield; $ETR(II)$, PSII relative electron transfer efficiency; $Y(NO)$, quantum production with dissipated energy; $Y(NPQ)$, quantum yield of regulated non-photochemical quenching in PSII; Fv/Fm , maximum potential light energy conversion efficiency of PSII; $n = 4$. Data were collected on days 15 and 30 of treatment. (D) Effects on gas exchange. A , net photosynthetic rate; E , transpiration rate; g_{H2O} , stomatal conductance; Ci , intercellular carbon dioxide concentration; CK, control; $-Fe$, Fe-deficient; $n = 4$. Data were collected on day 15 of treatment. ** $P < 0.01$ and * $P < 0.05$, treatment vs. control (t -test, FDR < 0.05).

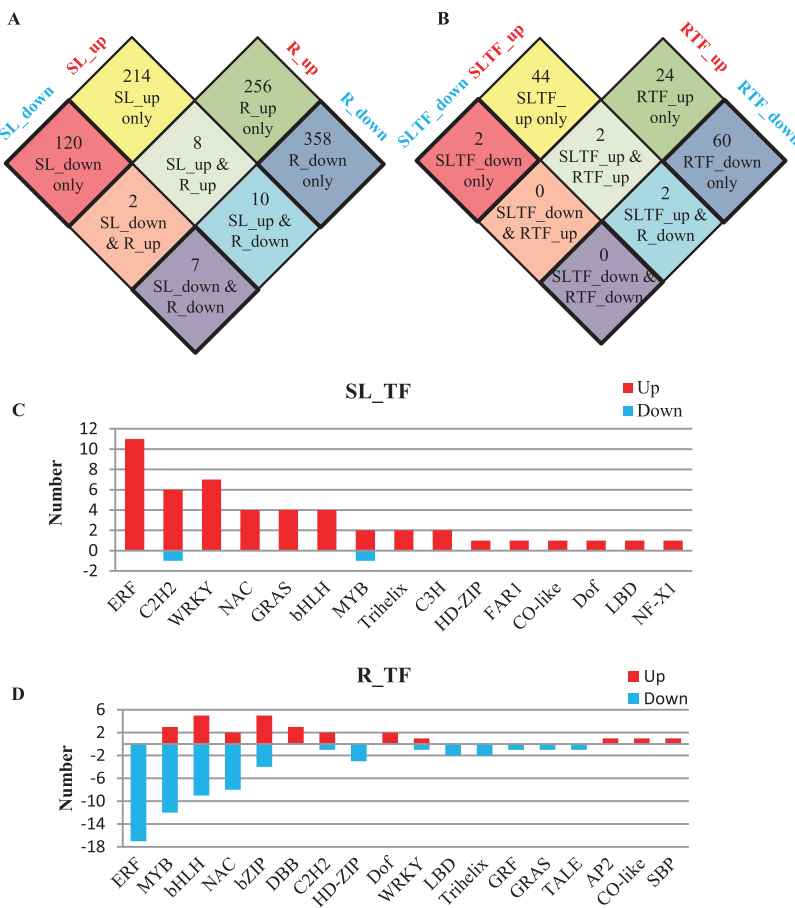


Figure 4. Analysis of DEGs and DETFs in the shoots and roots at the late stage of Fe deficiency. (A) Statistics for DEGs found in roots and shoots. (B) Statistics for DETFs found in roots and shoots. (C) Categories of DETF found in shoots. (D) Categories of DETF found in roots. SL_up, number of upregulated genes in the shoots; SL_down, number of downregulated genes in the shoots; R_up, number of upregulated genes in the roots; R_down, number of downregulated genes in the roots; SLTF_up, number of upregulated transcription factors in the shoots; SLTF_down, number of downregulated transcription factors in the shoots; RTF_up, number of upregulated transcription factors in the roots; RTF_down, number of downregulated transcription factors in the roots; SLTF, DETFs in the shoots; RTF, DETFs in the roots.

upregulated and 375 genes were downregulated. Only 27 DEGs were found in both the shoots and roots (Figure 4A). Of these 27 genes, 8 DEGs were upregulated and 7 DEGs were downregulated in both the shoots and roots. Ten DEGs were upregulated in the shoots while downregulated in the roots. Two DEGs were downregulated in the shoots, but upregulated in the roots. We randomly selected 6 of these 27 DEGs for qRT-PCR validation (Table 1). The qRT-PCR results showed that most selected genes were expressed differently between treatment and control groups, except for one gene (*Potri.016G124700*) in the roots ($P = 0.057$, t -test) and one gene (*Potri.012G055100*) in the shoots ($P = 0.066$, t -test). Although \log_2 FC values differed slightly between qRT-PCR and RNA-seq analyses, similar results were obtained for the six DEGs in both analyses, confirming the reliability of the RNA-seq results.

DETFs in the shoots and roots (Figure 4B) were identified using the Plant Transcription Factor Database (V4.0; <http://plantfdb.cbi.pku.edu.cn/>). In the shoots, a total of 50 DEGs belonging to

15 families were predicted to be DETFs. The top eight families were the ethylene response factor (ERF; 11 DEGs), C2H2 (7 DEGs), WRKY (7 DEGs), NAC (4 DEGs), bHLH (4 DEGs), GRAS (4 DEGs), MYB (3 DEGs) and C3H/Trihelix (2 DEGs), which accounted for 88.00% of total DEGs (Figure 4C, Table S2 available as Supplementary Data at *Tree Physiology Online*). In the roots, 88 DEGs in 18 transcription factor families were predicted to be DETFs. The top eight families were ERF (17 DEGs), MYB (15 DEGs), bHLH (14 DEGs), NAC (10 DEGs), bZIP (9 DEGs), HD-ZIP (3 DEGs), C2H2 (3 DEGs) and DBB (3 DEGs), which accounted for 84.09% of total DEGs (Figure 4D, Table S3 available as Supplementary Data at *Tree Physiology Online*). DETFs from the ERF, bHLH, NAC and MYB families were abundant in the shoots and roots, suggesting that these transcription factor families may contribute to the Fe-deficiency response. Of the 50 DETFs found in shoots, 48 were upregulated and 2 were downregulated (Figure 4C). Of the 88 DETFs found in roots, 26 were upregulated and 62 were downregulated (Figure 4D).

Table 1. Genes for qRT-PCR validation. *P*-values were calculated using independent *t*-test.

Gene ID	Description	RNA-seq Log ₂ FC	Shoots qRT-PCR Log ₂ FC	qRT-PCR <i>P</i> -value	RNA-seq Log ₂ FC	Roots qRT-PCR Log ₂ FC	qRT-PCR <i>P</i> -value
Potri.008G099900	Glutathione	2.14	8.85	0.006	2.72	7.32	0.035
Potri.012G055100	BTS, zinc finger BRUTUS-like	1.23	4.42	0.066	2.89	4.08	0.041
Potri.016G006500	OPT3, oligopeptide transporter 3	1.34	2.67	0.009	1.42	4.58	0.002
Potri.006G037600	<i>bHLH38/39</i> , iron ion homeostasis	1.16	10.13	0.008	3.49	4.58	0.025
Potri.006G103900	Ferritin precursor family	-1.89	-2.95	0.007	-2.95	-3.89	0.045
Potri.016G124700	Ferritin-chloroplastic-like	-2.67	-3.15	0.002	-3.15	-3.23	0.057

Our results indicate that most DEGs in the shoots were upregulated, whereas most DEGs in the roots were downregulated. Two *bHLH38/39* transcription factors, *Potri.006G037600* and *Potri.016G037300*, which positively regulate Fe homeostasis, were upregulated in both the shoots and roots. Two NAC-like transcription factors, *Potri.011G123300* and *Potri.005G069500*, which respond to Fe deficiency, were upregulated in the shoots and downregulated in the roots (see Tables S2 and S3 available as Supplementary Data at *Tree Physiology* Online). Other DETFs aside from *bHLH38/39* were involved in the regulation of Fe homeostasis in the roots, including FITs, PYE and ERF72. Two FITs, *Potri.009G005600* and *Potri.T155900*, and a PYE, *Potri.003G074400*, regulate Fe homeostasis positively. Conversely, ERF72 (*Potri.008G210900*) is involved in the negative regulation of Fe homeostasis. As in previous studies, *bHLH38/39* and PYE were upregulated and ERF72 was downregulated under Fe deficiency. Two FIT genes that were reported to be upregulated in *Arabidopsis* (Colangelo and Guerinot 2004, Yang et al. 2010) were downregulated in this study. Of the DETFs, three have been predicted to regulate the root or lateral root development, in addition to maintaining Fe balance. Of these three DETFs, *bHLH74* (*Potri.002G114700*), which positively regulates root development, was upregulated, whereas *WRKY75* (*Potri.001G328000*) and *MYB66* (*Potri.001G169600*), which inhibit root-hair formation, were downregulated (see Table S3 available as Supplementary Data at *Tree Physiology* Online).

Pathway enrichment analysis of DEGs in shoots and roots

According to the KEGG enrichment analysis, the DEGs in the shoots were enriched mainly in the porphyrin rings, the chlorophyll metabolism pathway, photosynthesis pathway and photosynthetic antenna proteins. The DEGs in the roots were largely enriched in the pathways for phenylpropanoid biosynthesis, ethylene synthesis and ethylene signal transduction (Figures 5 and 6). Six downregulated DEGs ($FC \leq 0.5$, $FDR < 0.05$) in the shoots were enriched in the chlorophyll synthesis pathway (Figure 5A, Table S4 available as Supple-

mentary Data at *Tree Physiology* Online). These DEGs included two glutamyl-tRNA reductase genes (*Potri.002G107800* and *Potri.009G080600*), a magnesium (Mg) chelatase gene (*Potri.006G051100*), two prochlorophyllate reductase genes (*Potri.001G403300* and *Potri.011G122400*) and a chlorophyll *b* reductase gene (*Potri.018G081200*). With use of a relaxed fold-change cutoff ($0.50 < FC \leq 0.67$, $FDR < 0.05$), another two Mg-protoporphyrin IX monomethyl cyclase genes (*Potri.016G025000* and *Potri.006G027300*) and a protoporphyrinogen-III oxidase gene (*Potri.002G186300*) were also found to be downregulated. The glutamyl-tRNA reductase and Mg chelatase genes produce two key enzymes in the chlorophyll synthesis pathway. Glutamyl-tRNA reductase catalyzes the synthesis of δ -amino- γ -levulinic acid, which is a rate-limiting step. Mg chelatase inserts Mg^{2+} into protoporphyrin IX, which is another critical step in chlorophyll synthesis (Adams et al. 2014). Therefore, Fe deficiency greatly suppresses chlorophyll synthesis in the shoots.

In the shoots, 26 DEGs ($FC \leq 0.5$, $FDR < 0.05$) that are involved in the photosynthetic pathway were downregulated (Figure 5B, Table S4 available as Supplementary Data at *Tree Physiology* Online). The downregulated DEGs involved in PSII activity included *LHCB1–6*, *PsbW*, *PsbY* and *PsbQ*. *LHCB1–6* encode the antenna proteins of PSII. *PsbW* and *PsbY* are small subunits in PSII. *PsbQ* is a subunit of the oxygen evolution complex (OEC). With use of a relaxed fold-change cutoff ($0.50 < FC \leq 0.67$, $FDR < 0.05$), the genes encode two other OEC subunits (*PsbO* and *PsbP*) and *PsbS*, which contributes to PSII stability, were also found to be downregulated (see Table S5 available as Supplementary Data at *Tree Physiology* Online). Electrons stored in P680 are transferred to PSI by the cytochrome b6f complex and plastocyanin (PC). The DEGs detected in this study did not include genes that encode the subunits of the cytochrome b6f complex. However, *petE*, which encodes PC, was downregulated. The downregulation of *petE* would affect photosynthetic electron transport efficiency and P700⁺ reduction. Other downregulated DEGs include *LHCA1*, which encodes the antenna light-harvesting

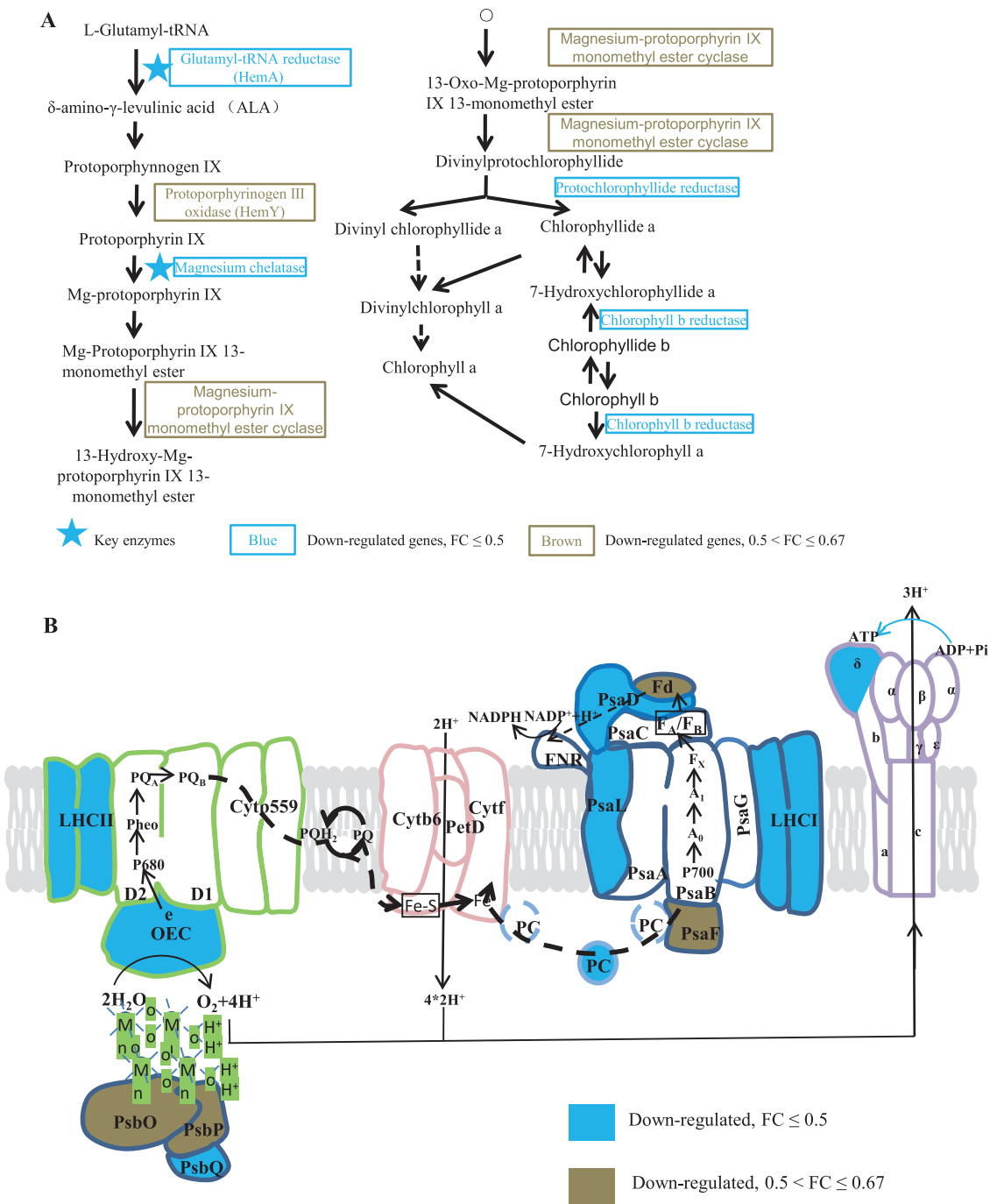


Figure 5. Pathway enrichment analysis of DEGs in shoots. (A) Shoot DEGs enriched in the chlorophyll synthesis pathway. (B) Shoot DEGs enriched in the photosynthesis pathway. LHCI, subunit of light harvesting complex of PSI; LHClI: subunit of light harvesting complex of PSII; OEC: oxygen evolution complex.

protein; *PsaD*, which encodes the ferredoxin-binding subunit; and genes that encode other PSI subunits (*psaE*, *psaK*, *psaL*, *psaN* and *psaO*). With use of a relaxed fold-change cutoff ($0.50 < \text{FC} \leq 0.67$, $\text{FDR} < 0.05$), *LHCA3*, an antenna protein-coding gene in PSI; *PsaF*, which is involved in the specific binding of plastocyanin; *petF*, which encodes ferredoxin that binds to PSI; and the gene that encodes the δ subunit of F-type ATP

synthase were also found to be downregulated (see Table S5 available as Supplementary Data at *Tree Physiology Online*). Therefore, Fe deficiency depresses photosynthetic activity in poplars.

All six DEGs related to the xylem synthesis pathway in the roots (Figure 6A, Table S6 available as Supplementary Data at *Tree Physiology Online*) were downregulated ($\text{FC} \leq 0.5$,

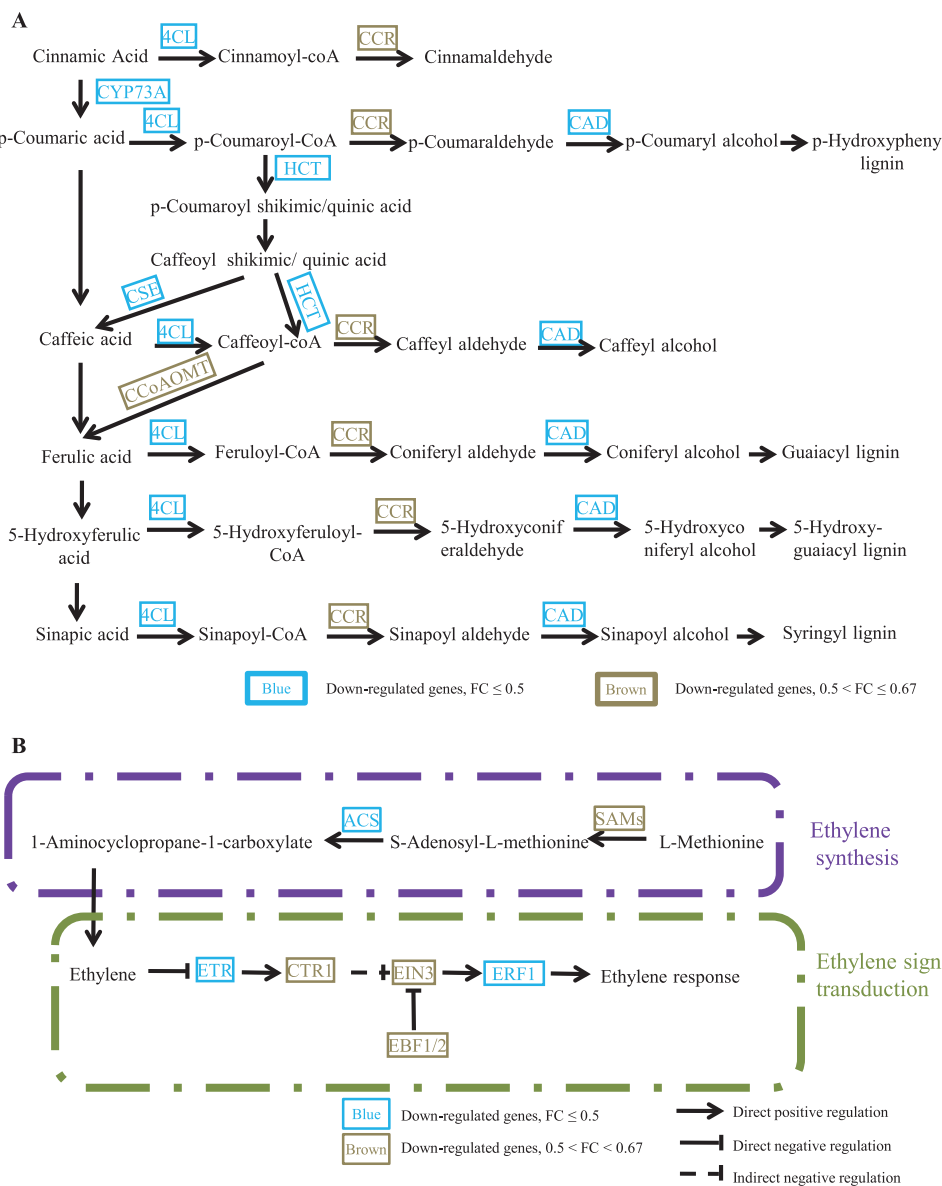


Figure 6. Pathway enrichment analysis of DEGs in roots. (A) Root DEGs enriched in the xylem synthesis pathway. (B) Root DEGs enriched in the ethylene synthesis and signal transduction pathways.

FDR < 0.05). These DEGs were a 4CL gene (*Potri.001G036900*), two CAD genes (*Potri.009G062800* and *Potri.001G463400*), a CYP73A gene (*Potri.019G130700*), an HCT gene (*Potri.003G183900*) and a CSE gene (*Potri.001G175000*). Four additional genes were found to be downregulated with use of a relaxed fold-change cutoff ($0.50 < FC \leq 0.67$, FDR < 0.05), including another 4CL gene (*Potri.003G188500*), a CCR gene (*Potri.003G181400*), a CAD gene (*Potri.009G063100*) and a CCoAOMT gene (*Potri.009G099800*). The downregulation of these genes would suppress the synthesis of lignin monomers, which might reduce lignin synthesis.

In the ethylene synthesis pathway in the roots, an ACS gene that encodes a key enzyme (*Potri.003G132300*) was down-

regulated. Two ethylene receptor genes (*Potri.008G164400* and *Potri.010G074300*) and two ethylene-responsive transcription factor (ERF1) genes (*Potri.008G166200* and *Potri.010G072300*) were also downregulated. With use of a relaxed fold-change cutoff ($0.50 < FC < 0.67$, FDR < 0.05), three SAMs genes on the ethylene synthesis pathway (*Potri.008G099300*, *Potri.013G004100* and *Potri.002G189000*), and EIN3 (*Potri.001G015900*), CTR1 (*Potri.006G115800*) and EBF1/2 (*Potri.018G027700*) on the ethylene signal transduction pathway, were found to be downregulated as well (Figure 6B, Table S7 available as Supplementary Data at *Tree Physiology Online*). Therefore, ethylene synthesis and signal transduction in the roots were inhibited by long-term Fe deprivation.

DEGs involved in the regulation of Fe homeostasis and Fe transport in shoots and roots

We identified the DEGs involved in the regulation of Fe homeostasis and Fe transport in the shoots and roots using GO annotation and data from previous studies (Tables 2 and 3). In the shoots and roots, *bHLH38/39* and *BTS* are common regulators of the response to Fe deficiency. Similar to results from previous studies, *bHLH38/39* and *BTS* were upregulated in the shoots and roots (Long et al. 2010). Additionally, *ERF72*, *FIT* and *PYE* were differentially expressed in the roots and contributed to the regulation of Fe homeostasis. Several genes involved in Fe uptake and transport in poplar were also differentially expressed. For example, in both the shoots and roots, *OPT3*, which is involved in the transport of Fe from the xylem to the phloem, was upregulated; *YSL3*, which encodes a transporter of the Fe^{3+} -nicotianamine chelate, was downregulated; and *VIT4*, which helps to transport Fe from the cytosol to the vacuole, was downregulated (Tables 2 and 3). *IRT1* was upregulated in

the shoots (Table 2). In the roots, *NARMP1*, which encodes an Fe^{2+} transporter, was upregulated; a *CCC1*-related gene (*Potri.012G004000*) that encodes a protein that transports cytoplasmic Fe and Mn into the vacuole was downregulated; and two FCR coding genes (*FRO2* and *FRO-like*) were upregulated (Table 3). FCR activity was 54.29% higher in Fe-deficient roots than in control roots (see Figure S1 available as Supplementary Data at *Tree Physiology Online*). This result indicates that, like other nongraminaceous plants such as *Arabidopsis thaliana* and *Trifolium pretense* L (Yi and Guerinot 1996, Jin et al. 2008), poplars could induce *FRO2* in response to Fe deficiency.

Discussion

Fe deficiency has different morphological effects on shoots and roots

Interveinal chlorosis in young leaves is a typical symptom of Fe deficiency. After 15 days under Fe-deficient conditions, the

Table 2. DEGs involved in iron transport and regulation in shoots. DEGs with $\text{FC} \geq 2$ ($\text{Log}_2\text{FC} \geq 1$) or $\text{FC} \leq 0.5$ ($\text{Log}_2\text{FC} \leq -1$) are shown (FDR < 0.05).

Process	Gene ID	Description	Log_2FC	FDR
Transcriptional regulation	Potri.016G037300	<i>bHLH38/39</i> , iron ion homeostasis	2.10	4.53E-11
	Potri.006G037600	<i>bHLH38/39</i> , iron ion homeostasis	1.16	1.82E-06
	Potri.012G055100	<i>BTS</i> , zinc finger BRUTUS-like	1.23	4.22E-06
Iron uptake and transport	Potri.015G117900	<i>IRT1</i> , Fe^{2+} transport 1-like	6.55	3.10E-05
	Potri.016G006500	<i>OPT3</i> , oligopeptide transporter 3	1.34	2.86E-10
	Potri.012G024700	<i>YSL3</i> , metal-nicotianamine transporter YSL3-like	-1.21	0.04
	Potri.002G069400	<i>VIT4</i> , vacuolar iron transporter homolog 4-like	-3.36	1.24E-03

Table 3. DEGs involved in iron transport and regulation in roots. DEGs with $\text{FC} \geq 2$ ($\text{Log}_2\text{FC} \geq 1$) or $\text{FC} \leq 0.5$ ($\text{Log}_2\text{FC} \leq -1$) are shown (FDR < 0.05).

Process	Gene ID	Description	Log_2FC	FDR
Transcriptional regulation	Potri.012G055100	<i>BTS</i> , zinc finger BRUTUS-like	2.89	1.33E-17
	Potri.006G037600	<i>bHLH38/39</i> , iron ion homeostasis	3.49	1.79E-08
	Potri.016G037300	<i>bHLH38/39</i> , iron ion homeostasis	2.66	9.62E-05
	Potri.003G074400	<i>PYE</i> , transcription factor bHLH47-like	1.20	2.00E-03
	Potri.T155900	<i>FER/FIT</i> , FER-like transcription factor	-1.41	1.13E-04
	Potri.009G005600	<i>FER/FIT</i> , FER-like transcription factor	-1.87	2.80E-07
	Potri.008G210900	<i>ERF72</i> , ethylene-responsive transcription factor RAP2-3-like	-2.12	1.83E-12
Iron uptake and transport	Potri.005G181100	<i>Nramp1</i> , metal transporter Nramp1-like	9.46	2.82E-13
	Potri.005G181000	<i>Nramp1</i> , metal transporter Nramp1-like	7.26	5.14E-07
	Potri.006G006000	<i>OPT3</i> , oligopeptide transporter 3	1.84	2.66E-11
	Potri.016G006500	<i>OPT3</i> , oligopeptide transporter 3	1.42	1.03E-08
	Potri.012G024700	<i>YSL3</i> , metal-nicotianamine transporter YSL3-like	-1.00	0.01
	Potri.012G027800	<i>YSL3</i> , metal-nicotianamine transporter YSL3-like	-1.22	0.04
	Potri.005G190800	<i>VIT4</i> , vacuolar iron transporter homolog 4-like	-2.06	0.01
	Potri.012G004000	Fe/Mn transmembrane transporter, CCC1-related family	-2.12	0.04
	Potri.002G069400	<i>VIT4</i> , vacuolar iron transporter homolog 4-like	-3.64	4.15E-12
	Potri.018G106000	<i>VIT4</i> , vacuolar iron transporter homolog 4-like	-5.64	1.93E-11
	Potri.014G088000	<i>FRO2</i> , ferric reduction oxidase 2-like	5.59	1.39E-20
	Potri.001G079000	ferric reduction oxidase chloroplastic-like	1.30	1.08E-03

top three leaves of treatment plants became obviously chlorotic (Figure 1A). Fe-deficient plants were also shorter than Fe-sufficient plants. Hence, Fe deficiency can inhibit shoot growth. Fe deficiency affects root morphology as well. Fe-deficient individuals of poplars had significantly longer root lengths and more roots. Fe deficiency has been shown to promote the development of root hairs and lateral roots in plants (Graziano and Lamattina 2007). Thus, robust root systems are produced to improve Fe acquisition when plants are Fe deficient. Nevertheless, if the Fe supply is insufficient to meet the physiological and metabolic requirements of the shoots, shoot growth will be inhibited.

Fe deficiency inhibits chlorophyll synthesis and photosynthesis

The results from the transcriptomic and physiological analyses verified that Fe deficiency suppresses chlorophyll synthesis. The genes that encode two key enzymes (glutamyl-tRNA reductase and Mg chelatase) and that encode proteins in the chlorophyll synthesis pathway (protochlorophyllide reductase, chlorophyll *b* reductase, Mg-protoporphyrin IX monomethyl ester cyclase and protoporphyrinogen-III oxidase were downregulated. Thus, Fe deficiency substantially inhibited chlorophyll synthesis in poplar. Fe deficiency led to decreases in chlorophyll and carotenoid concentrations. However, the ratio of chlorophyll *a* to *b* was not affected by Fe deficiency. Chlorophyll *b* and carotenoids are auxiliary pigments that collect light energy and transmit it to the antenna pigment during photosynthesis. A portion of chlorophyll *a* can become antenna pigment and directly participate in the photochemical reaction. As Fe deficiency results in the reduction of photosynthetic pigment levels, light-energy capture and photochemical reactions become less efficient, and photosynthetic rates are greatly affected.

In the photosynthesis pathway, 26 major genes that code for subunits in the light system were downregulated. In PSII, *LHCB1–6*, which code for antenna light-harvesting proteins 1–6, and OEC-coding genes were downregulated. Therefore, Fe deficiency inhibited the stability of the PSII complex and its light-harvesting and oxygen-emitting abilities. In PSI, *LHCA1*, *PsaD* and *PsaF* were downregulated. *LHCA1* encodes an antenna light-harvesting protein, *PsaD* is involved in ferredoxin binding, and *PsaF* is involved in the specific binding of plastocyanin. The downregulation of these genes indicates that the light-capturing and electron-transfer capabilities of PSI were inhibited. The genes that encode the δ subunit of F-type ATP synthase and OEC subunits, which are involved in photosynthetic phosphorylation, were downregulated. This downregulation might reduce the amount of H⁺ released from water in the thylakoid cavity. Consequently, pH gradients, which drive ATP synthesis, would not be formed and the rates of photosynthetic phosphorylation would decrease. The measurement of photosynthetic parameters indicated that Fe deficiency limits PSI and PSII. However,

the effects on two photosystems were not synchronized. The Y (I) and ETR (I) of PSI were significantly lower in treatment plants after 15 days of Fe deficiency, whereas the Y (II) and ETR (II) of PSII did not differ significantly between the treatment and control groups. The Y (II) and ETR (II) of treated plants were significantly lower than those of control plants only after 30 days of treatment. Therefore, PSI was affected by Fe deficiency earlier than PSII. This perhaps because PSI contains more Fe atoms than does PSII. Under Fe deficiency, the decrease in chlorophyll levels and photosynthetic activity reduces light-energy capture and photochemical and electron-transfer efficiency. Fe deficiency also greatly reduces photosynthetic activity in poplar.

Fe deficiency increases Mn, Cu and Zn content in roots

Fe deficiency significantly reduced Fe content in the roots, stems and leaves of poplars. However, Mn, Cu and Zn content increased significantly in the roots, similar to results of previous studies (Jin et al. 2017). Divalent metal ion transporters are likely non-specific. They transport not only Fe²⁺, but also Mn²⁺, Cu²⁺ and Zn²⁺. For example, IRT1 is known to transport both Fe²⁺ and Zn²⁺ (Vert et al. 2002), and NRAMP1 transports both Fe²⁺ and Mn²⁺ (Curie et al. 2000). Because the acquisition of Fe was promoted, the absorption capacity for Mn, Cu and Zn in the roots also increased. Nevertheless, Mn, Cu and Zn content in the shoots did not change significantly. Thus, the shoot: root ratios of Mn, Cu and Zn content decreased.

Regulation of the response mechanism in roots at the late stage of Fe deficiency

In *Arabidopsis*, ethylene is involved in regulating responses to Fe deficiency. The ethylene biosynthesis and signaling pathways are affected within 24 h of Fe deficiency in *Arabidopsis* (Garcia et al. 2010). *EIN3* and *EIL1*, which belong to the ethylene signal transduction pathway, interact with *FIT* proteins, which are transcription factors that regulate Fe homeostasis, to prevent *FIT* degradation by proteases (Lingam et al. 2011). In this study, we detected the responses to Fe deficiency in poplars at the late stage of treatment, when chlorosis occurred. The DEGs in the ethylene synthesis and signal transduction pathways were all downregulated (Figure 6B). In the ethylene synthesis pathway, the genes encoding ACS and SAMs were both downregulated ($0.50 < FC \leq 0.67$, $FDR < 0.05$). In the ethylene signal transduction pathway, *EIN3*, a gene regulating Fe homeostasis ($FC = 0.61$, $FDR < 0.01$), and 17 *ERFs* were downregulated. Additionally, *FIT*, which is regulated by *EIN3/EIL1*, was downregulated. These results contrast with those obtained in studies of *Arabidopsis*. We hypothesize that the inhibition of the ethylene-regulated *FIT* network may be due to negative feedback from downstream genes or products. However, this hypothesis requires further verification. Among the 17 downregulated *ERFs*, *ERF72* has been shown to negatively regulate the response to Fe deficiency in *Arabidopsis*. *AtERF72* suppresses

AtIRT1 and *AtAHA2* expression (Liu et al. 2017). Thus, a decrease in *ERF72* expression improves Fe uptake. At the late stage of Fe deficiency, the FIT network in the roots was inhibited, but the PYE regulatory network remained active to maintain Fe homeostasis in the roots. In the PYE regulatory network, *BTS*, which is an Fe sensor in dicotyledonous plants, is involved in the response to Fe deficiency, and *BTS* is upregulated during Fe deficiency (Long et al. 2010, Kobayashi and Nishizawa 2014, Selote et al. 2015). *BTS* and its downstream genes, such as *PYE* and *bHLH38/39*, were consistently upregulated in this study. *FIT* and *bHLH38/39* form a heterodimer with each other, which induces *FRO2* and *IRT1* at the transcriptional and post-transcriptional levels, respectively (Yuan et al. 2008). Therefore, we speculate that *IRT1* expression may be upregulated at the early stage of Fe deficiency in poplars. At the late stage

of deficiency, the inhibition of *FIT* expression subsequently decreased *IRT1* expression. Upregulated *PYE* directly inhibits the expression of *ZIF1*, a gene encoding vacuolar membrane facilitator that maintaining Zn²⁺ concentration in vacuoles. This inhibition may be a mechanism for detoxification in plants. Under Fe deficiency, this detoxification mechanism could prevent excessive Zn²⁺ from accumulating in plants. *PYE* also promotes root growth and development, which enhances Fe uptake (Long et al. 2010). Hence, at the late stage of Fe deficiency, the PYE regulation network, rather than the FIT regulation network, played positive role in maintaining Fe homeostasis.

The roots of poplars respond to Fe deficiency in three major ways: Fe uptake, Fe redistribution and root development (Figure 7). For Fe uptake, *FRO2*, which is involved in the reduction of Fe³⁺ to Fe²⁺, was upregulated (Figures 7 and 8).

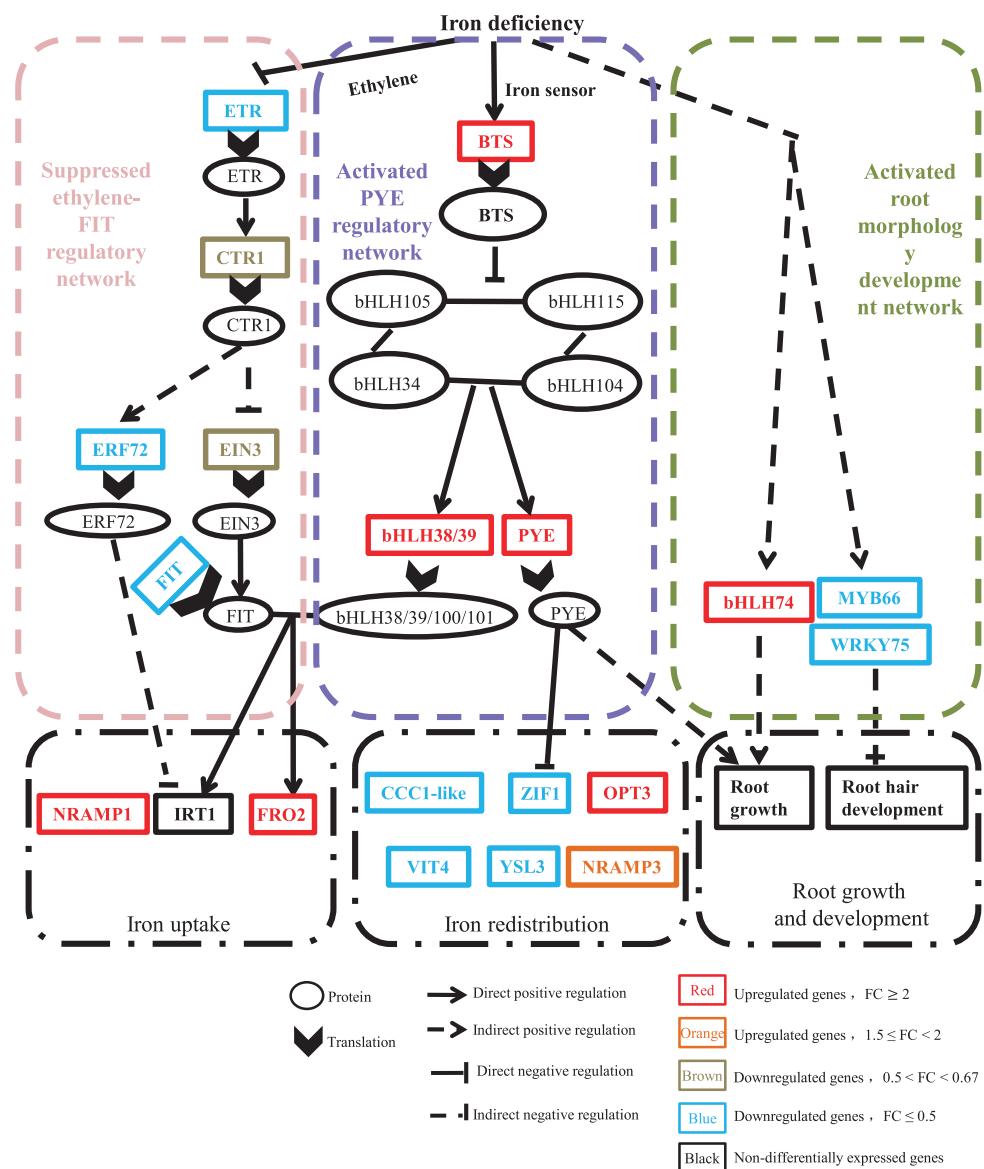


Figure 7. Network for the regulation of iron deficiency in poplar roots.

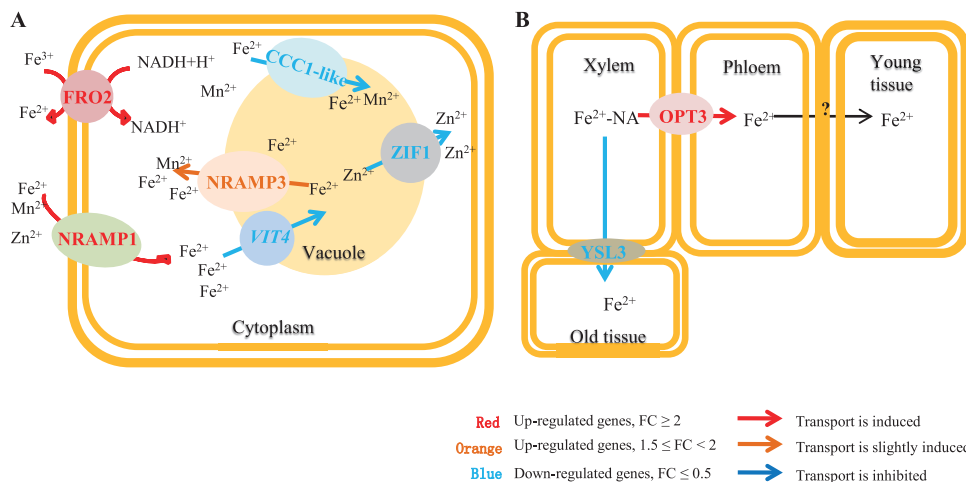


Figure 8. Iron transport in poplar roots under iron-deficiency stress. (A) Iron uptake and intracellular transport in the roots. (B) Inter-organizational transport in the roots.

At the late stage of Fe deficiency, only *NRAMP1*, one of the genes encoding Fe²⁺ transporters, was upregulated. *IRT1*, the well-known gene encoding the main transporter for Fe²⁺ uptake, was not differentially expressed in the roots. *NRAMP1* and *IRT1* have redundancy in function and both transporters absorb Fe²⁺ on the plasma membrane in *Arabidopsis* (Cailliatte et al. 2010, Castaings et al. 2016). Our results indicate that at the late stage of Fe deficiency, Fe uptake in the roots of poplars depends on *NRAMP1*, rather than *IRT1*. In terms of Fe redistribution at the intracellular level (Figure 8), *NRAMP3* was upregulated and *VIT4* and *CCC1-related* were downregulated. Thus, Fe stored in the vacuole was exported as much as possible to the cytoplasm to meet basic metabolic requirements. At the tissue level, *OPT3* expression was induced, and Fe was transported to younger tissues to increase Fe use rates. *YSL3* expression was inhibited to prevent the transport of Fe to neighboring senescent tissues, avoiding Fe waste. In terms of morphology, Fe-deficient individuals of poplars had longer and more roots than did control individuals, which was consistent with results from the transcriptomic analysis of the roots. The overexpression of *bHLH74* in *Arabidopsis* has been shown to result in root elongation (Bao et al. 2014). *WRKY75* suppresses the development of root hairs in the non-root hair files of *Arabidopsis* (Rishmawi et al. 2014). *MYB66* is a major transcription factor that inhibits the proliferation of root hair cells (Yao et al. 2013). In poplar, *bHLH74* was upregulated, whereas *WRKY75* and *MYB66* were downregulated (Figure 7), similar to results from studies of *Arabidopsis*.

Conclusion

In summary, Fe deficiency inhibited plant growth, chlorophyll synthesis and photosynthesis in poplars. Of the two photosystems, PSI was affected by Fe deficiency earlier than PSII. At

the late stage of Fe deficiency, genes in the ethylene-regulated FIT network were inhibited in the roots, whereas genes in the PYE regulatory network continued to actively regulate Fe homeostasis. Additionally, poplars can respond to Fe deficiency by promoting root growth and development.

Accession numbers

High-throughput sequence data generated from this study have been deposited in the Gene Expression Omnibus (GEO) database under accession number GSE116838.

Supplementary Data

Supplementary Data for this article are available at *Tree Physiology* online.

Funding

This study was supported by the Chinese Academy of Forestry (CAFYBB2018ZX002) and the National Natural Science Foundation of China (31500547 and 31425006).

References

- Adams NB, Marklew CJ, Brindley AA, Hunter CN, Reid JD (2014) Characterization of the magnesium chelatase from *Thermosynechococcus elongatus*. *Biochem J* 457:163–170.
- Bao M, Bian H, Zha Y, Li F, Sun Y, Bai B, Chen Z, Wang J, Zhu M, Han N (2014) miR396a-mediated basic helix-loop-helix transcription factor *bHLH74* repression acts as a regulator for root growth in *Arabidopsis* seedlings. *Plant Cell Physiol* 55:1343–1353.
- Briat JF, Dubois C, Gaymard F (2015) Iron nutrition, biomass production, and plant product quality. *Trends Plant Sci* 20:33–40.
- Bruinsma J (1963) The quantitative analysis of chlorophylls a and b in plant extracts. *Photochem Photobiol* 2:241–249.

- Cailliatte R, Schikora A, Briat JF, Mari S, Curie C (2010) High-affinity manganese uptake by the metal transporter NRAMP1 is essential for *Arabidopsis* growth in low manganese conditions. *Plant Cell* 22: 904–917.
- Castaings L, Caquot A, Loubet S, Curie C (2016) The high-affinity metal transporters NRAMP1 and IRT1 team up to take up iron under sufficient metal provision. *Sci Rep* 6:37222–37232.
- Colangelo Aksoy E, Jeong IS, Koiwa H (2013) Loss of function of *Arabidopsis* C-terminal domain phosphatase-like1 activates iron deficiency responses at the transcriptional level. *Plant Physiol* 161:330–345.
- Colangelo EP, Guerinot ML (2004) The essential basic helix-loop-helix protein FIT1 is required for the iron deficiency response. *Plant Cell* 16:3400–3412.
- Curie C, Alonso JM, Le, Jean M, Ecker JR, Briat JF (2000) Involvement of NRAMP1 from *Arabidopsis thaliana* in iron transport. *Biochem J* 347:749–755.
- Curie C, Briat JF (2003) Iron transport and signaling in plants. *Annu Rev Plant Biol* 54:183–206.
- Einset J, Winge P, Bones AM, Connolly EL (2008) The FRO2 ferric reductase is required for glycine betaine's effect on chilling tolerance in *Arabidopsis* roots. *Physiol Plant* 134:334–341.
- Gao YQ, Chao DY (2016) Get more acids for more iron: a new regulatory pathway for iron homeostasis. *Mol Plant* 9:498–500.
- Garcia MJ, Lucena C, Romera FJ, Alcantara E, Perez-Vicente R (2010) Ethylene and nitric oxide involvement in the up-regulation of key genes related to iron acquisition and homeostasis in *Arabidopsis*. *J Exp Bot* 61:3885–3899.
- Gollhofer J, Schlawicke C, Jungnick N, Schmidt W, Buckhout TJ (2011) Members of a small family of nodulin-like genes are regulated under iron deficiency in roots of *Arabidopsis thaliana*. *Plant Physiol Biochem* 49:557–564.
- Gollhofer J, Timofeev R, Lan P, Schmidt W, Buckhout TJ (2014) Vacuolar-iron-transporter1-like proteins mediate iron homeostasis in *Arabidopsis*. *PLoS One* 9:e110468–e110475.
- Graziano M, Lamattina L (2007) Nitric oxide accumulation is required for molecular and physiological responses to iron deficiency in tomato roots. *Plant J* 52:949–960.
- Hindt MN, Akmakjian GZ, Pivarski KL, Punshon T, Baxter I, Salt DE, Guerinot ML (2017) BRUTUS and its paralogs, BTS LIKE1 and BTS LIKE2, encode important negative regulators of the iron deficiency response in *Arabidopsis thaliana*. *Metallomics* 9:876–890.
- Hirayama T, Lei GJ, Yamaji N, Nakagawa N, Ma JF (2018) The putative peptide gene FEP1 regulates iron deficiency response in *Arabidopsis*. *Plant Cell Physiol* 59:1739–1752. (doi: [10.1093/pcp/pcy145](https://doi.org/10.1093/pcp/pcy145)).
- Huang D, Dai W (2015a) Molecular characterization of the basic helix-loop-helix (bHLH) genes that are differentially expressed and induced by iron deficiency in *Populus*. *Plant Cell Rep* 34:1211–1224.
- Huang D, Dai W (2015b) Two iron-regulated transporter (IRT) genes showed differential expression in poplar trees under iron or zinc deficiency. *J Plant Physiol* 186–187:59–67.
- Ivanov R, Brumbarova T, Bauer P (2012) Fitting into the harsh reality: regulation of iron-deficiency responses in dicotyledonous plants. *Mol Plant* 5:27–42.
- Jin CW, Chen WW, Meng ZB, Zheng SJ (2008) Iron deficiency-induced increase of root branching contributes to the enhanced root ferric chelate reductase activity. *J Integr Plant Biol* 50:1557–1562.
- Jin CW, You GY, He YF, Tang C, Wu P, Zheng SJ (2007) Iron deficiency-induced secretion of phenolics facilitates the reutilization of root apoplastic iron in red clover. *Plant Physiol* 144:278–285.
- Jin LF, Liu YZ, Du W, Fu LN, Hussain SB, Peng SA (2017) Physiological and transcriptional analysis reveals pathways involved in iron deficiency chlorosis in *fragrant citrus*. *Tree Genet Genomes* 13: 51–60.
- Kobayashi T, Nishizawa NK (2012) Iron uptake, translocation, and regulation in higher plants. *Annu Rev Plant Biol* 63:131–152.
- Kobayashi T, Nishizawa NK (2014) Iron sensors and signals in response to iron deficiency. *Plant Sci* 224:36–43.
- Lanquar V, Lelievre F, Bolte S et al. (2005) Mobilization of vacuolar iron by AtNRAMP3 and AtNRAMP4 is essential for seed germination on low iron. *EMBO J* 24:4041–4051.
- Li X, Zhang H, Ai Q, Liang G, Yu D (2016) Two bHLH transcription factors, bHLH34 and bHLH104, regulate iron homeostasis in *Arabidopsis thaliana*. *Plant Physiol* 170:2478–2493.
- Ling HQ, Bauer P, Bereczky Z, Keller B, Ganap M (2002) The tomato fer gene encoding a bHLH protein controls iron-uptake responses in roots. *Proc Natl Acad Sci U S A* 99:13938–13943.
- Lingam S, Mohrbacher J, Brumbarova T, Potuschak T, Fink-Straube C, Blondet E, Genschik P, Bauer P (2011) Interaction between the bHLH transcription factor FIT and ETHYLENE INSENSITIVE3/ETHYLENE INSENSITIVE3-LIKE1 reveals molecular linkage between the regulation of iron acquisition and ethylene signaling in *Arabidopsis*. *Plant Cell* 23:1815–1829.
- Liu W, Li Q, Wang Y, Wu T, Yang Y, Zhang X, Han Z, Xu X (2017) Ethylene response factor AtERF72 negatively regulates *Arabidopsis thaliana* response to iron deficiency. *Biochem Biophys Res Commun* 491:862–868.
- Livak KJ, Schmittgen TD (2001) Analysis of relative gene expression data using real-time quantitative PCR and the $2^{-\Delta\Delta CT}$ method. *Methods* 25:402–408.
- Long TA, Tsukagoshi H, Busch W, Lahner B, Salt DE, Benfey PN (2010) The bHLH transcription factor POPEYE regulates response to iron deficiency in *Arabidopsis* roots. *Plant Cell* 22:2219–2236.
- Marschner H, Romheld V, Kissel M (1986) Different strategies in higher plants in mobilization and uptake of iron. *J Plant Nutr* 9: 695–713.
- Rishmawi L, Pesch M, Juengst C, Schauss AC, Schrader A, Hulskamp M (2014) Non-cell-autonomous regulation of root hair patterning genes by WRKY75 in *Arabidopsis*. *Plant Physiol* 165:186–195.
- Robinson NJ, Procter CM, Connolly EL, Guerinot ML (1999) A ferric-chelate reductase for iron uptake from soils. *Nature* 397: 694–697.
- Selote D, Samira R, Matthiadis A, Gillikin JW, Long TA (2015) Iron-binding E3 ligase mediates iron response in plants by targeting basic helix-loop-helix transcription factors. *Plant Physiol* 167:273–286.
- Storey JD, Bass AJ, Dabney A, Robinson D (2015) qvalue: Q-value estimation for false discovery rate control, R package version 2.10.0.
- Thomine S, Lelievre F, Debarbieux E, Schroeder JI, Barbier-Brygoo H (2003) AtNRAMP3, a multispecific vacuolar metal transporter involved in plant responses to iron deficiency. *Plant J* 34:685–695.
- Toselli M, Marangoni B, Tagliavini M (2000) Iron content in vegetative and reproductive organs of nectarine trees in calcareous soils during the development of chlorosis. *Eur J Agron* 13:279–286.
- Varotto C, Maiwald D, Pesaresi P, Jahns P, Salamini F, Leister D (2002) The metal ion transporter IRT1 is necessary for iron homeostasis and efficient photosynthesis in *Arabidopsis thaliana*. *Plant J* 31: 589–599.
- Vert G, Grotz N, Dedaldechamp F, Gaynard F, Guerinot ML, Briat JF, Curie C (2002) IRT1, an *Arabidopsis* transporter essential for iron uptake from the soil and for plant growth. *Plant Cell* 14: 1223–1233.
- Wang N, Cui Y, Liu Y, Fan H, Du J, Huang Z, Yuan Y, Wu H, Ling HQ (2013) Requirement and functional redundancy of lb subgroup bHLH proteins for iron deficiency responses and uptake in *Arabidopsis thaliana*. *Mol Plant* 6:503–513.
- Waters BM, Chu HH, Didonato RJ, Roberts LA, Easley RB, Lahner B, Salt DE, Walker EL (2006) Mutations in *Arabidopsis* yellow

- stripe-like1 and yellow stripe-like3 reveal their roles in metal ion homeostasis and loading of metal ions in seeds. *Plant Physiol* 141: 1446–1458.
- Yang TJ, Lin WD, Schmidt W (2010) Transcriptional profiling of the *Arabidopsis* iron deficiency response reveals conserved transition metal homeostasis networks. *Plant Physiol* 152:2130–2141.
- Yao H, Wang G, Guo L, Wang X (2013) Phosphatidic acid interacts with a MYB transcription factor and regulates its nuclear localization and function in *Arabidopsis*. *Plant Cell* 25:5030–5042.
- Yi Y, Guerinot ML (1996) Genetic evidence that induction of root Fe (III) chelate reductase activity is necessary for iron uptake under iron deficiency. *Plant J* 10:835–844.
- Yuan Y, Wu H, Wang N, Li J, Zhao W, Du J, Wang D, Ling HQ (2008) FIT interacts with AtbHLH38 and AtbHLH39 in regulating iron uptake gene expression for iron homeostasis in *Arabidopsis*. *Cell Res* 18:385–397.
- Zhai Z, Gayomba SR, Jung HI et al. (2014) OPT3 is a phloem-specific iron transporter that is essential for systemic iron signaling and redistribution of iron and cadmium in *Arabidopsis*. *Plant Cell* 26:2249–2264.
- Zhang J, Liu B, Li M, Feng D, Jin H, Wang P, Liu J, Xiong F, Wang J, Wang HB (2015) The bHLH transcription factor bHLH104 interacts with IAA-LEUCINE RESISTANT3 and modulates iron homeostasis in *Arabidopsis*. *Plant Cell* 27:787–805.